# Photodegradation of methylmercury in stream ecosystems

Martin Tsz Ki Tsui,[a,*] Joel D. Blum,[a] Jacques C. Finlay,[b] Steven J. Balogh,[c] Sae Yun Kwon,[a] and Yabing H. Nollet[c]

[a] Department of Earth and Environmental Sciences, University of Michigan, Ann Arbor, Michigan
[b] Department of Ecology, Evolution, and Behavior, University of Minnesota, St. Paul, Minnesota
[c] Metropolitan Council Environmental Services, St. Paul, Minnesota

### Abstract

   Photodegradation is an important sink for highly toxic methylmercury (MeHg) in aquatic ecosystems. Lakes have been extensively studied for MeHg photodegradation, but much less is known about streams, mainly because of the heterogeneity in sunlight availability along stream reaches and because there has been a lack of tools with which to integrate this longitudinal variability. We utilize odd-mass anomalies of stable Hg isotopes (i.e., $\Delta^{199}Hg$) as a proxy for estimating the relative extent of MeHg photodegradation in streams. In a northern California stream network, levels of MeHg in water and biota increased with increasing stream size in headwater and intermediate streams (drainage areas ranging from 0.6 to 150 km$^2$), but MeHg levels decreased substantially in larger streams (drainage areas up to 1212 km$^2$). In smaller streams, the increase of MeHg levels is attributed to increasing in situ MeHg production and is accompanied by only a small increase in $\Delta^{199}Hg$, indicating that the rate of MeHg photodegradation is low relative to the rate of in situ MeHg production. In larger streams, decreasing MeHg levels coincided with significant increases in $\Delta^{199}Hg$ of MeHg (an average increase of 1.5‰ ± 0.5‰, $n = 4$), indicating that increasing MeHg photodegradation reduced MeHg levels in these wider, more open channels. Our findings clearly indicate that increasing sunlight availability in stream channels substantially increases MeHg photodegradation, which can reduce MeHg contamination in stream food webs.

   Mercury (Hg) is a global contaminant as a result of its long-range atmospheric transport and widespread deposition (Fitzgerald et al. 1998). Most deposited Hg is inorganic [Hg(0) or Hg(II)], and a small fraction of that may be microbially converted into highly toxic methylmercury (MeHg) (Benoit et al. 2003). In aquatic food webs, MeHg can extensively bioaccumulate and biomagnify, often leading to levels in fish that are unsafe for human and wildlife consumption (Wiener et al. 2003). The ecosystem production of MeHg is widely considered to be critical in determining Hg bioavailability and thus the exposure of humans and wildlife. Processes that degrade MeHg act to counterbalance MeHg production, representing important controls on steady-state levels of MeHg in the environment (Benoit et al. 2003). MeHg can be degraded microbially and photochemically (Sellers et al. 1996; Benoit et al. 2003), with photodegradation (PD) widely regarded as the dominant sink for MeHg in aquatic ecosystems such as lakes (Sellers et al. 1996; Hammerschmidt and Fitzgerald 2006).

   Previous lake studies (Sellers et al. 1996; Hammerschmidt and Fitzgerald 2006) quantified rates of MeHg PD by in situ incubation of MeHg-spiked lake water in closed bottles under the water surface with exposure to sunlight. Rates of MeHg PD were found to be first order with respect to irradiance and MeHg concentration (Sellers et al. 1996; Hammerschmidt and Fitzgerald 2006). Recent studies (Lehnherr and St. Louis 2009; Black et al. 2012) found that ultraviolet (UV, including UVA and UVB) is the most important wavelength of sunlight for MeHg PD, and, therefore, the rate of MeHg PD typically decreases

rapidly with lake depth as a result of the attenuation of UV by dissolved organic matter (DOM) (Laurion et al. 2000; Hammerschmidt and Fitzgerald 2006). However, the underlying mechanism of MeHg PD is not completely clear. The currently proposed mechanisms of MeHg PD include (1) hydroxyl radicals generated by the photo-Fenton reaction (Hammerschmidt and Fitzgerald 2010) and (2) singlet oxygen generated by sunlight reacting with DOM (Zhang and Hsu-Kim 2010). Indeed, multiple reaction pathways for MeHg PD are likely, but their relative importance may change with ambient factors such as water chemistry (e.g., DOM, salinity) and sunlight wavelength (Black et al. 2012).

   Similar to lakes, food webs in natural streams without point sources (e.g., mining and industrial discharge) are often widely contaminated by MeHg through atmospheric deposition (Peterson et al. 2007), especially in forested watersheds with extensive wetland cover (Chasar et al. 2009). In montane watersheds without wetlands and point sources, in situ production of MeHg has been shown to provide a substantial load of MeHg for the stream food webs (Tsui et al. 2010). Intuitively, MeHg PD should be particularly important in streams because of their shallow depth and rapid mixing. Therefore, the higher irradiance per unit volume of water should produce a higher extent of MeHg PD in streams compared to lakes. We thus expect that factors affecting sunlight availability in the water column in streams would also affect MeHg PD: for example, (1) the type of stream habitat (e.g., fast-flowing riffles, slow-flowing shallows and deep pools; Bradley et al. 2011); (2) the canopy cover along stream reaches (Finlay 2011); and (3) the characteristics of stream water (e.g., DOM, suspended particles) that can attenuate UV radiation (Laurion et al. 2000). However, the quantification of

---

MeHg PD in streams is challenging. The unidirectional flow in streams leads to MeHg PD occurring over the length of the stream reaches, and, thus, the incubation approach used for lake studies at fixed positions (Sellers et al. 1996; Hammerschmidt and Fitzgerald 2006) is not appropriate. In fact, whether the rates of MeHg PD measured by the incubation approach are close to natural levels is also questionable because the incubated water does not circulate and mix, and the bottle materials (e.g., Teflon) can attenuate part of the sunlight spectrum (Lehnherr and St. Louis 2009; Black et al. 2012). For streams, heterogeneity of canopy cover as well as different water depths in different stream reaches further complicates in situ measurement of stream MeHg PD. Thus, new approaches that integrate this heterogeneity and estimate MeHg PD over space and time are needed for fast-flowing streams as a result of the difficulties and uncertainties discussed above.

The recent development of methods for precise analysis of stable Hg isotopes provides a new avenue for examining MeHg PD in aquatic ecosystems (e.g., Blum 2011). Mass-independent fractionation (MIF) of odd-mass isotopes of Hg ($^{199}$Hg and $^{201}$Hg) is mainly caused by photochemical reactions, and the odd-mass anomalies of Hg isotopes in MeHg (i.e., $\Delta^{199}$Hg or $\Delta^{201}$Hg) have been found to be proportional to the fraction of MeHg PD in aquatic systems (Bergquist and Blum 2007). Large positive MIF (e.g., $\Delta^{199}$Hg > 0.5‰) has been observed in many environmental samples that contain predominantly MeHg, such as fish muscle (Bergquist and Blum 2007) and bird eggs (Point et al. 2011). Since MIF of MeHg isotopes is thought to be negligible during trophic transfer processes (Kwon et al. 2012), odd-mass anomalies of Hg isotopes in MeHg measured in food webs should reflect the extent to which MeHg PD occurred in the ambient environment prior to bioaccumulation of the remaining or non-photodegraded MeHg (Blum 2011).

In this study we measured stable Hg isotopes in stream insect larvae at different positions in a stream network in northern California and used $\Delta^{199}$Hg to estimate the degree (or percentage) of MeHg PD using an experimentally derived relationship (Bergquist and Blum 2007). The main structural variability among sites in the stream network is increasing channel width and, thus, decreasing canopy cover (from 98% to 0%) along the drainage gradient. Sunlight availability increases downstream, resulting in increasing algal abundance with stream size (Finlay 2004; Finlay et al. 2011). Stream nutrient chemistry also changes longitudinally in the study network as a result of increasing biological metabolism downstream, including increasing levels of dissolved nitrogen caused by increasing cyanobacteria abundance and decreasing levels of dissolved silica caused by increasing diatom abundance (Finlay et al. 2011). However, this longitudinal variation in nutrient chemistry should not produce major effects on MeHg PD, as might large changes in DOM and suspended particles. Longitudinal changes in DOM and suspended particles were very small in this stream network during summer baseflow (Finlay 2004; Tsui et al. 2009). We thus hypothesized that MeHg PD would increase downstream as a result of decreasing canopy cover or increasing sunlight availability

and that this would be reflected in the longitudinal pattern of MIF of stable Hg isotopes in bioaccumulated MeHg.

## Methods

*Study sites and sample collection*—Our study sites were within or near the Angelo Coast Range Reserve (39′44″N, 123′39″W) in Mendocino County, California, where most precipitation falls between October and April. After winter rains, decreases in discharge begin in May and continue through late August, and stream productivity typically peaks during midsummer (Finlay 2004; Finlay et al. 2011). In July 2011, we surveyed nine sites (drainage area [DA] from 0.6 to 1212 km$^2$) in the forested headwaters and the main channels of the South Fork Eel (SFE) River (Fig. 1). As the channel widens, canopy cover decreases (from 98% to 0%), and sunlight penetration increases, leading to generally increasing water temperature and algal productivity (Finlay 2004), which is similar to that associated with other temperate watersheds (Finlay 2011). Throughout this article we used DA as a proxy of stream size, following the pattern of previous studies in this stream network (Finlay 2004; Tsui et al. 2009; Finlay et al. 2011).

At each site, we collected water samples into two acid-cleaned 500 mL Teflon bottles, which were then transported on ice to the field station. Water in one of the bottles was filtered to < 0.45 $\mu$m, and both unfiltered and filtered fractions were immediately preserved with 0.4% trace metal–grade hydrochloric acid (Tsui et al. 2010). Bottle blanks containing Milli-Q ultrapure water (18.2 M$\Omega$) were below the method detection limit (20 pg L$^{-1}$) for MeHg and 16–27 pg L$^{-1}$ for total Hg (THg). We found that filtration did not significantly elevate THg or MeHg levels in the water samples. Also, we collected four dominant functional feeding groups (FFGs) of stream insect larvae (i.e., scrapers: *Glossosoma* and *Neophylax*; collectors: *Heptagenia* and *Nixe*; filterers: *Hydropsyche*; and predators: *Hesperoperla* and *Calineuria*). Insect larvae were transported alive in a cooler at ~ 15°C and processed at the field station as previously described (Tsui et al. 2009). All biological samples were pooled samples of multiple individuals (typically 20 to 200) within each site in order to allow us to obtain an adequate amount of Hg for precise stable Hg isotope measurements (at least 6 ng of total Hg, or THg). Biological samples from the two smallest tributaries (i.e., McKinley Creek and Skunk Creek) were combined (named 'McKinley and Skunk Creek'; DA = 0.6 km$^2$) for stable Hg isotope measurements because of the difficulty of collecting adequate samples in these small, unproductive streams. Thus, there are a total of eight sites for comparison of Hg isotope ratios. Overall, only scraper samples were found to be inadequate for Hg isotope analyses at two sites (i.e., SFE River at Garberville [DA = 1212 km$^2$] and McKinley and Skunk Creek [DA = 0.6 km$^2$]) because of the small number of scraper samples collected, but they were adequate for Hg concentration analyses.

*Hg concentration analyses*—For THg, water samples were oxidized with 1% BrCl at 60°C overnight (Tsui et al. 2010) and neutralized with hydroxylamine, and THg was
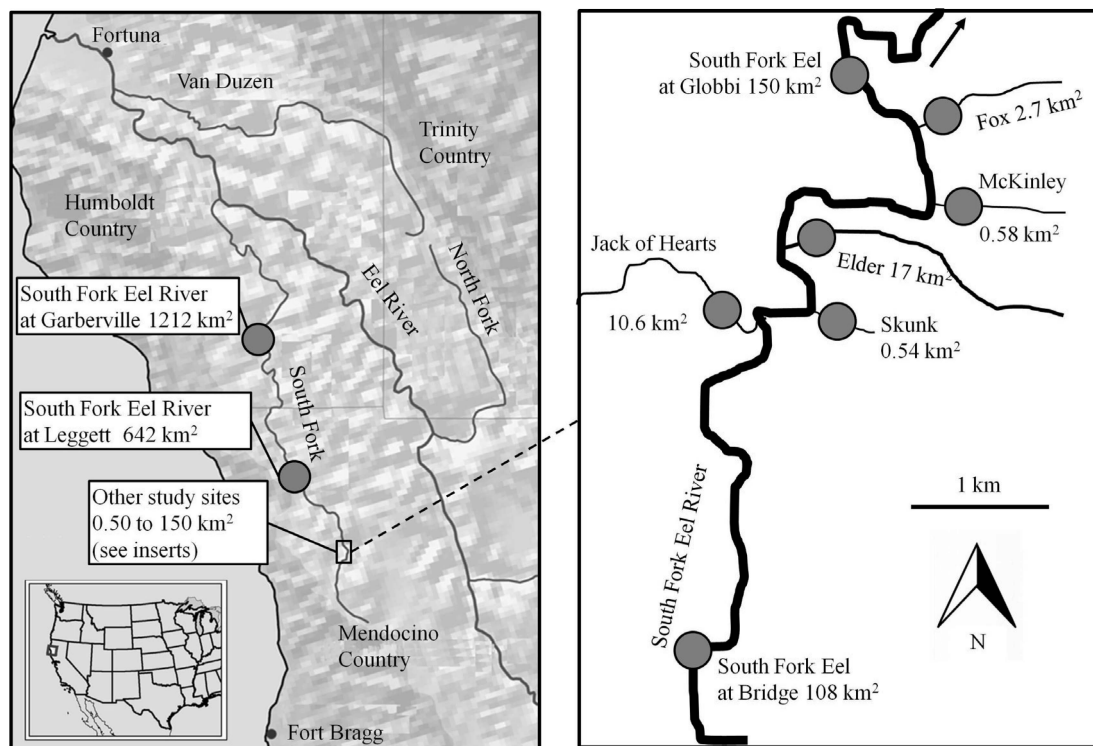
Fig. 1. Map showing locations of sample collection (denoted by circle symbols, with values of drainage area) along the SFE River in northern California (eight sites in Mendocino County and one site in Humboldt County), with map showing locations of smaller streams in the inserts on the right. Original source of map on the left: http://en.wikipedia.org/wiki/South_Fork_Eel_River.

quantified by single-amalgamation cold vapor atomic fluorescence spectrometry (CVAFS) (Liang and Bloom 1993). Duplicate analyses of water samples yielded an average percent difference of 4.8% (range: 0.9–9.6%, $n$ = 3). For MeHg, acidified water samples were distilled to remove matrix that could cause interference, adjusted to pH 4.9 by acetate buffer, ethylated by sodium tetraethylborate, purged onto Tenax traps by Hg-free $N_2$ gas, and then MeHg was quantified by CVAFS after being separated by a gas chromatography column at 105°C and pyrolyzed at 700–800°C (Bloom 1989; Horvat et al. 1993). Water samples spiked with MeHg (as fish protein certified reference material for trace metals; National Research Council Canada [NRCC] DORM-3, digested in KOH–methanol) prior to distillation yielded an average recovery of 102% (range: 91–109%, $n$ = 6). For water samples having MeHg below the method detection limit (i.e., 20 pg $L^{-1}$), we assigned a value of half the detection limit (i.e., 10 pg $L^{-1}$) for graphical presentation.

All biological samples were freeze-dried, ground, and homogenized using an acid-cleaned glass mortar and pestle. Samples were digested with 4.6 mol $L^{-1}$ $HNO_3$ at 60°C for 12 h, and an aliquot of each digest was analyzed for MeHg by CVAFS (Hammerschmidt and Fitzgerald 2005). Remaining samples were completely oxidized by a mixture of 5% $KMnO_4$ and 5% $K_2S_2O_8$ (1:1, v:v) at room temperature for subsequent THg analyses (Tsui et al. 2009). Throughout the digestion of biological samples, we included reagent blanks and two standard reference materials (SRMs; i.e., National Institute of Standards and

Technology [NIST] 2976 mussel tissue and NRCC TORT-2 lobster hepatopancreas). The reagent blanks consistently showed nondetectable levels of MeHg and an average of 2.8 pg $mL^{-1}$ of THg. For MeHg, the recoveries ranged from 96% to 115% for NIST 2976 ($n$ = 4) and from 98% to 110% for NRCC TORT-2 ($n$ = 6). For THg, the recoveries ranged from 90% to 110% for NIST 2976 ($n$ = 4) and from 96% to 111% for NRCC TORT-2 ($n$ = 6). A subset of biological samples were run in duplicate, and the average percentage difference was 9.7% ($n$ = 19) for MeHg and 1.9% ($n$ = 30) for THg.

*Stable mercury (Hg) isotope analyses*—All biological samples were thermally combusted in a two-stage quartz tube furnace, and released Hg(0) was trapped by bubbling through 1% $KMnO_4$ solution, as previously described (Biswas et al. 2008; Gehrke et al. 2011; Kwon et al. 2012). We further separated sample Hg from the combustion matrix by reduction with $SnCl_2$ and reoxidation with another 1% $KMnO_4$ solution. Prior to the isotope measurements, the final Hg concentrations of the samples were adjusted to a constant level ($\pm$ 5%) along with Hg bracketing standards (SRM NIST 3133) for each mass spectrometry run session (Blum and Bergquist 2007; Biswas et al. 2008; Gehrke et al. 2011). Stable Hg isotope ratios were measured using a Nu Instruments multicollector inductively coupled plasma mass spectrometer following methods previously described (Bergquist and Blum 2007; Biswas et al. 2008; Gehrke et al. 2011). Mass-dependent fractionation (MDF) of Hg isotopes is reported as $\delta^{202}$Hg

in permil (‰) referenced to SRM NIST 3133. MIF of Hg isotopes is the difference between the measured $\delta^{202}$Hg value and that which would be predicted based on mass dependence. The mass-independent Hg isotope composition is reported as either $\Delta^{199}$Hg or $\Delta^{201}$Hg in ‰. Isotopic compositions are calculated according to Blum and Bergquist (2007) as

$$\delta^{202}\text{Hg} = \tag{1}$$
$$\{[(^{202}\text{Hg} \div {}^{198}\text{Hg})_{\text{sample}} \div ({}^{202}\text{Hg} \div {}^{198}\text{Hg})_{\text{NIST3133}}] - 1\} \times 1000$$

$$\Delta^{201}\text{Hg} \approx \delta^{201}\text{Hg}_{\text{measured}} - (\delta^{202}\text{Hg}_{\text{measured}} \times 0.752) \tag{2}$$

$$\Delta^{199}\text{Hg} \approx \delta^{199}\text{Hg}_{\text{measured}} - (\delta^{202}\text{Hg}_{\text{measured}} \times 0.252) \tag{3}$$

Analytical uncertainty was monitored by replicate analyses of a secondary standard, University of Michigan (UM)–Almadén, and replicate combustions and analyses of NRCC TORT-2 at different final Hg concentrations (0.75–5.0 ng g$^{-1}$). Because isotope analyses of different samples were conducted at different final Hg concentrations, we established and employed the external analytical reproducibility (2 SD) for $\Delta^{199}$Hg at different ranges of final Hg concentration by measurements of NRCC TORT-2 as $\pm$ 0.06‰ for $\Delta^{199}$Hg (2 SD, $n = 8$) for 4.8–5.0 ng g$^{-1}$, $\pm$ 0.10‰ for $\Delta^{199}$Hg (2 SD, $n = 11$) for 1.9–2.9 ng g$^{-1}$, and $\pm$ 0.24‰ for $\Delta^{199}$Hg (2 SD, $n = 7$) for 0.75–1.3 ng g$^{-1}$.

*Estimation of MeHg isotope values and MeHg PD*—It should be noted that current methods for high-precision stable Hg isotope measurements are limited to analysis of THg in environmental samples (Blum 2011). Because Hg(II) and MeHg often have contrasting Hg isotopic compositions in the same environment (Gantner et al. 2009; Senn et al. 2010; Gehrke et al. 2011), it is important to consider the isotopic composition of MeHg if we want to estimate system-specific MeHg PD (Bergquist and Blum 2007; Point et al. 2011; Perrot et al. 2012). All insect samples have variable fractions of THg as MeHg (i.e., $f_{\text{MeHg}}$), and therefore $f_{\text{MeHg}}$ can significantly influence the THg isotope values of $\Delta^{199}$Hg (MIF). Thus, we found it necessary to estimate MeHg isotope values ($\Delta^{199}$Hg). Recently, it was found that Hg(II) in the SFE River (at DA of 150 km$^2$) had a $\Delta^{199}$Hg value close to zero (i.e., $-0.1$‰) (Tsui et al. 2012), which is similar to $\Delta^{199}$Hg values of environmental samples with predominantly Hg(II), such as sediments (Gantner et al. 2009; Senn et al. 2010; Gehrke et al. 2011), coals, and soils (Biswas et al. 2008). We used the following equation to estimate $\Delta^{199}$Hg of MeHg (abbreviated as $\Delta^{199}$Hg$_{\text{MeHg}}$):

$$\Delta^{199}\text{Hg}_{\text{MeHg}} = \left[\Delta^{199}\text{Hg} - \left(f_{\text{Hg(II)}} \times \Delta^{199}\text{Hg}_{\text{Hg(II)}}\right)\right] \div f_{\text{MeHg}} \tag{4}$$

where $f_{\text{Hg(II)}} + f_{\text{MeHg}} = 1.0$; $\Delta^{199}$Hg$_{\text{Hg(II)}}$ was assumed to be relatively constant across the watershed and to have a value of $-0.10$‰.

We also estimated the percentage of MeHg photodegraded before being bioaccumulated at each of our study sites, using the relationship generated from a previous
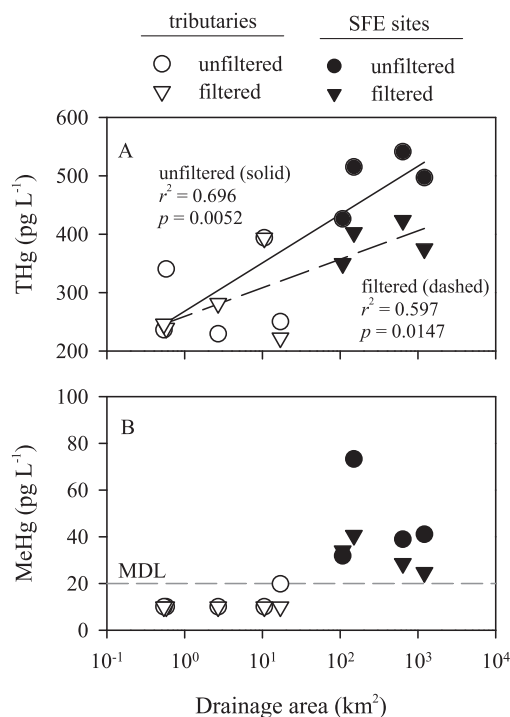


Fig. 2. Spatial variation of concentrations of (A) THg and (B) MeHg in unfiltered and filtered fractions of stream water in the stream network. (A) Linear regression analyses were performed for both unfiltered and filtered fractions. (B) Horizontal dashed line indicates method detection limit (MDL) of MeHg at 20 pg L$^{-1}$. Note: Samples with nondetects were plotted at a value of half the detection limit.

MeHg PD laboratory experiment conducted at a DOM concentration of 1 mg C L$^{-1}$ under natural sunlight (Bergquist and Blum 2007) (note: DOM in stream water among our study sites during baseflow was close to or below 1 mg C L$^{-1}$; Finlay et al. 2011). The percentage of MeHg PD (i.e., %PD) is calculated according to the following equation adapted from Bergquist and Blum (2007):

$$\%\text{PD} = \tag{5}$$
$$\left(1 - e\left\{\left[10^3 \times \ln\left(10^{-3} \times \Delta^{199}\text{Hg}_{\text{MeHg}} + 1\right)\right] \div -3.33\right\}\right) \times 100$$

*Statistical analysis*—Linear regression analyses were performed by SigmaPlot 7.0 (Systat), and the significance level was set at $p < 0.05$.

## Results

*Hg concentrations in water*—In the stream network, filtered THg levels were uniformly low (0.24–0.54 ng L$^{-1}$) (Fig. 2A), approaching the low end among temperate streams in North America (Brigham et al. 2009). Unfiltered THg levels increased strongly with stream size (Fig. 2A), which we speculate is a result of increasing levels of fine particles ($> 0.45$ $\mu$m) in the water derived from biological
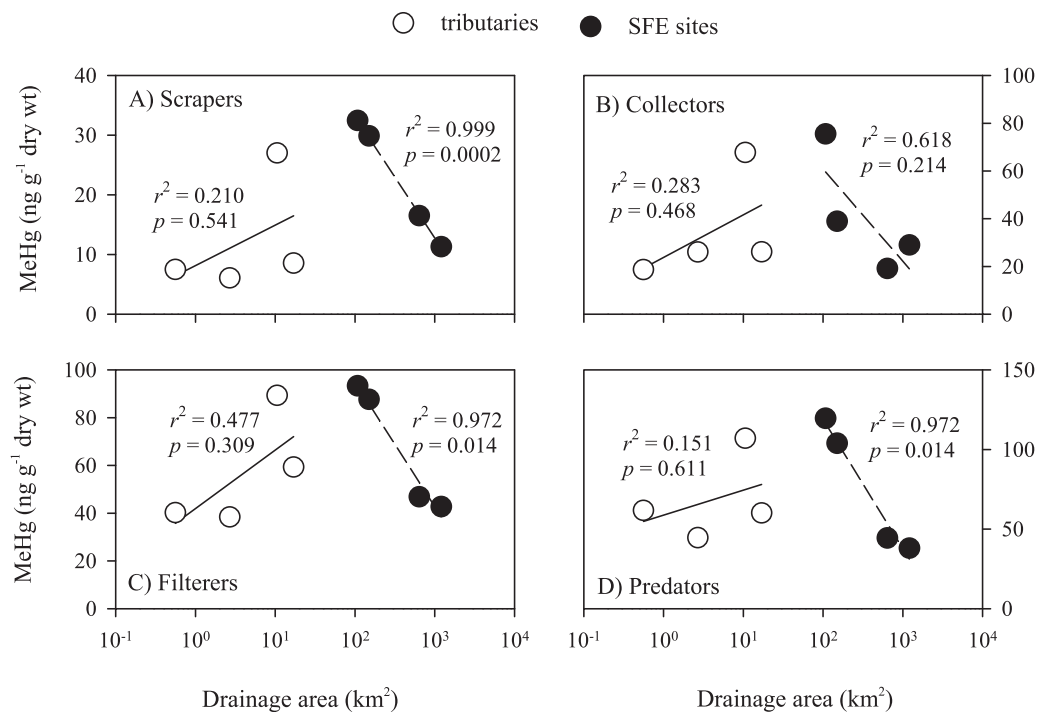
Fig. 3. Spatial variation of MeHg concentrations in four FFGs of invertebrates: (A) scrapers (armored caddisflies: *Glossosoma* and *Neophylax*); (B) gatherer-collectors (flathead mayflies: *Heptagenia* and *Nixe*); (C) particle filterers (net-spinning caddisflies: *Hydropsyche*); and (D) invertebrate predators (perlidae stoneflies: *Calineuria* and *Hesperoperla*). Two linear regression analyses were carried out for each FFG: Solid lines for streams with drainage area from 0.56 to 17 km² (tributaries); dashed lines for streams with drainage area from 108 to 1212 km² (SFE sites).

processing of algal and detrital materials in upstream sections (Wallace and Webster 1996). We found undetectable levels ($< 20$ pg $L^{-1}$) of MeHg (both unfiltered and filtered) in upstream tributaries (DA $< 10$ km²), and MeHg levels were close to or slightly above 20 pg $L^{-1}$ (method detection limit) for midsize streams (DA between 10 and 20 km²) (Fig. 2B). For larger sites in the SFE River (DA from 108 to 1212 km²) MeHg levels were considerably above the method detection limit and ranged from 32 to 73 pg $L^{-1}$ for unfiltered stream water and from 25 to 41 pg $L^{-1}$ for filtered stream water (Fig. 2B). In this study, we sampled two sites draining larger basins in the SFE River (DA = 642 and 1212 km²) (Fig. 1), but we found lower MeHg concentrations in water at these sites (average decreases by 24% for unfiltered and 29% for filtered fraction) compared to sites of smaller DA at the SFE River that were sampled (DA = 108 and 150 km²) (Fig. 2B).

*Hg concentrations in biota*—Among sites there were large variations in concentrations of THg (total range: 12–139 ng $g^{-1}$ dry weight) and MeHg (total range: 6–120 ng $g^{-1}$ dry weight) in all stream insect larvae. There were also large variations in MeHg concentrations between the four FFGs at individual sites, with the lowest being scrapers (total range of MeHg: 6–32 ng $g^{-1}$ dry weight) and the highest being invertebrate predators (total range of MeHg: 38–120 ng $g^{-1}$ dry weight) (Fig. 3A–D), which is consistent with MeHg biomagnification along the food chain (Wiener et al. 2003). Here, we focus on MeHg because it is the bioaccumulative and biomagnifying form of Hg (Wiener

et al. 2003). Spatially there were weak increases of MeHg concentrations in biota with stream size in tributaries (DA from 0.6 to 17 km²), which is consistent with a previous observation in the stream network (Tsui et al. 2009). MeHg concentrations in biota were much higher in SFE sites at DA of 108 and 150 km², but significant decreases in MeHg bioaccumulation occurred downstream in sites with DA of 642 and 1212 km² (Fig. 3A–D), in parallel with the spatial gradient of MeHg levels in stream water as described above (Fig. 2B). Interestingly, we found that the fraction of THg as MeHg (i.e., $f_{MeHg}$) in the invertebrates changed longitudinally and followed the spatial patterns of MeHg levels in the water and biota (Fig. 4).

*Stable isotopes of MeHg and MeHg photodegradation*— In order to provide a comparison of stable Hg isotopes among invertebrate FFGs across the eight sites, we estimated the isotopic compositions of bioaccumulated MeHg (*see* Methods). With the exception of one small tributary (Fox Creek, DA = 2.7 km²), $\Delta^{199}Hg_{MeHg}$ appeared to increase gradually downstream within each FFG for streams with DA values ranging from 0.6 to 17 km² (Fig. 5A–D). However, $\Delta^{199}Hg_{MeHg}$ values increased significantly downstream among the four sites at the SFE River with DA values ranging from 108 to 1212 km² (Fig. 5A–D). Similar to previous aquatic studies (Senn et al. 2010; Gehrke et al. 2011; Perrot et al. 2012), the MIF of Hg isotopes in this study appears to be caused by the magnetic isotope effect. Previous studies found a slope between $\Delta^{199}Hg$ and $\Delta^{201}Hg$ of 1.36 for MeHg in a
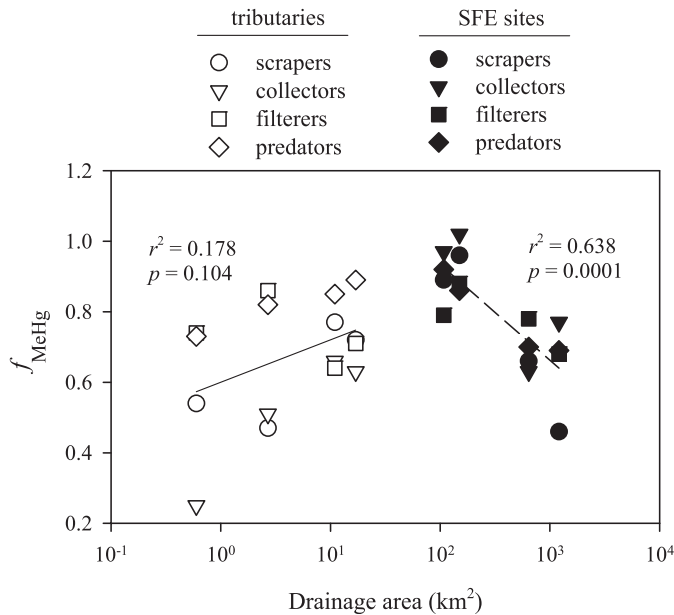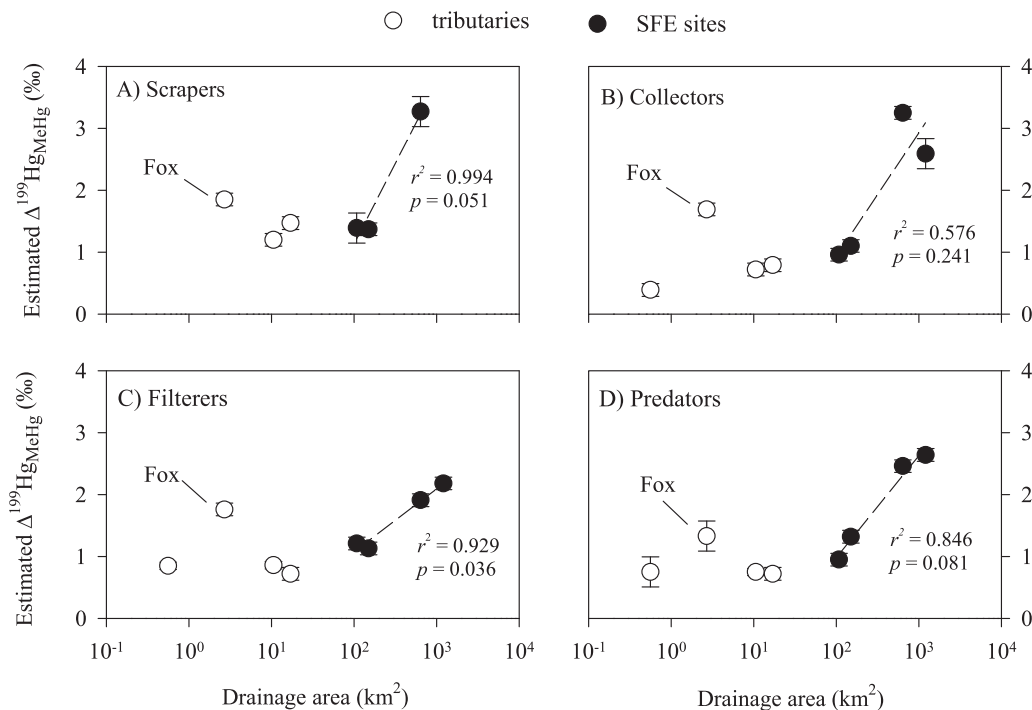
Fig. 4. Spatial variation of fraction of THg as MeHg (i.e., $f_{MeHg}$) in four FFGs of invertebrates: scrapers (armored caddisflies: *Glossosoma* and *Neophylax*), gatherer-collectors (flathead mayflies: *Heptagenia* and *Nixe*), particle filterers (net-spinning caddisflies: *Hydropsyche*), and invertebrate predators (perlidae stoneflies: *Calineuria* and *Hesperoperla*). Two linear regression analyses were carried out for all FFGs: Solid line for streams with drainage area from 0.56 to 17 km² (tributaries); dashed line for streams with drainage area from 108 to 1212 km² (SFE sites).

laboratory-controlled MeHg PD experiment (Bergquist and Blum 2007).

Our study shows an overall slope between $\Delta^{199}Hg$ and $\Delta^{201}Hg$ of $1.21 \pm 0.046$ (SE) (Fig. 6), which is lower than 1.36 but similar to those values identified in other studies of fish (e.g., 1.20 in northern Gulf of Mexico [Senn et al. 2010]; 1.26 in San Francisco Bay [Gehrke et al. 2011]; 1.27 in Lake Baikal in Russia [Perrot et al. 2012]). Figure 7A shows the relationship between daily light flux above the water surface in mid–summer 2008 (Finlay, 2011) and canopy cover across the study stream network (DA: 0.2–150 km²). As shown, sunlight availability only increased weakly with reduction in canopy cover (from 98% to 79%) among tributaries but increased strongly with reduction in canopy cover (from 43% to 25%) among sites in the SFE River (Fig. 7A). Similarly, we found a positive relationship between %MeHg PD (estimated from $\Delta^{199}Hg_{MeHg}$) and canopy cover among both tributaries and SFE sites (Fig. 7B).

## Discussion

In this study we observed longitudinal changes in MeHg levels in water and biota and $f_{MeHg}$ in biota along a drainage gradient (Figs. 2–4). Specifically, we observed weak increases of MeHg levels in small and intermediate streams (DA: 0.6–17 km²) but clearly decreasing trends in MeHg levels in larger channels (DA: 108–1212 km²). We also found increasing $\Delta^{199}Hg_{MeHg}$ values along the drainage gradient (except for Fox Creek; Fig. 5), with a strongly negative relationship with canopy cover (Fig. 7B).



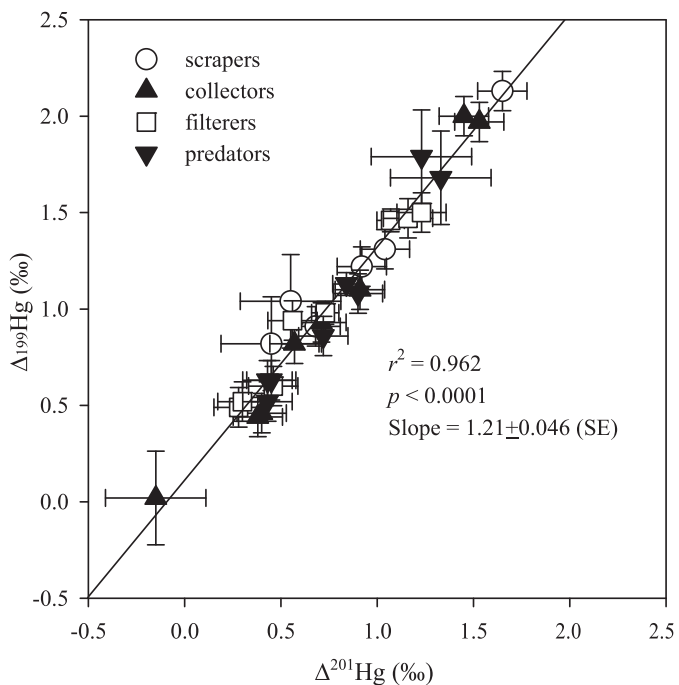Fig. 5. Spatial variation of estimated $\Delta^{199}Hg_{MeHg}$ in four FFGs of invertebrates: (A) scrapers (armored caddisflies: *Glossosoma* and *Neophylax*); (B) gatherer-collectors (flathead mayflies: *Heptagenia* and *Nixe*); (C) particle filterers (net-spinning caddisflies: *Hydropsyche*); and (D) invertebrate predators (perlidae stoneflies: *Calineuria* and *Hesperoperla*). Linear regression analyses were performed for each FFG only in SFE sites. Data points for Fox Creek are specified. There are no isotope data for scrapers in streams with drainage areas of 0.6 and 1212 km². Error bars represent external analytical reproducibility (2 SD).

Fig. 6. Relationship between $\Delta^{199}Hg$ and $\Delta^{201}Hg$ of all insect larvae samples (legends separated by FFGs). Linear regression analyses were performed for all samples. Error bars represent analytical reproducibility (2 SD).



Fig. 7. (A) Relationship between mean daily light flux in mid–summer 2008 and canopy cover in sites (including sites not studied for Hg isotope ratios) across the stream network. Light measurements were performed at individual sites from 8:00 h through 18:00 h daily for 1–2 weeks (Finlay 2011). (B) Relationship between mean % MeHg PD (estimated from $\Delta^{199}Hg_{MeHg}$) and canopy cover in sites across the stream network. For both graphs, Fox Creek is indicated. Two linear regression analyses were carried out: Solid lines for streams with drainage areas from 0.56 to 17 km$^2$ (tributaries); dashed lines for streams with drainage areas from 108 to 1212 km$^2$ (SFE sites). Data points represents the averages of the different FFGs; error bars are SD ($n = 3$–4).

These results indicate that the 'net' balance between the production and degradation of MeHg (especially PD) within channels changes longitudinally and results in the observed spatial variability of MeHg levels in water and biota with stream size during summer baseflow.

Compared to MeHg levels in other stream ecosystems, MeHg concentrations in water and insect larvae in our study watershed were relatively low. For example, across a land cover gradient in the south to north direction of eastern Minnesota it was observed that filtered MeHg concentrations in stream water during summer baseflow ranged from $< 40$ to 470 pg L$^{-1}$; the high values were observed mainly in streams located in watersheds with high percentage covers of forest and wetland in northern Minnesota (Tsui and Finlay 2011). In the current study, MeHg concentrations in the filtered water ranged only from $< 20$ to 41 pg L$^{-1}$; we attribute the low aqueous levels of MeHg to low DOM levels in these streams, due mainly to the absence of wetlands in the study watershed. In the Minnesota study, MeHg concentrations in an organism from the filterer FFG, hydropsychid caddisflies, ranged from 13 to 220 ng g$^{-1}$ (Tsui and Finlay 2011), but MeHg concentrations in this filterer ranged from 38 to 93 ng g$^{-1}$ in the current study. MeHg concentrations in water and biota of other FFGs in this study are comparable to or lower than those of samples analyzed in a large-scale study examining eight streams across the United States (in Florida, Wisconsin, and Oregon) (Brigham et al. 2009; Chasar et al. 2009). Therefore, we expect that Hg cycling in our study watershed is biogeochemically similar to that of other watersheds receiving primarily atmospheric deposition.
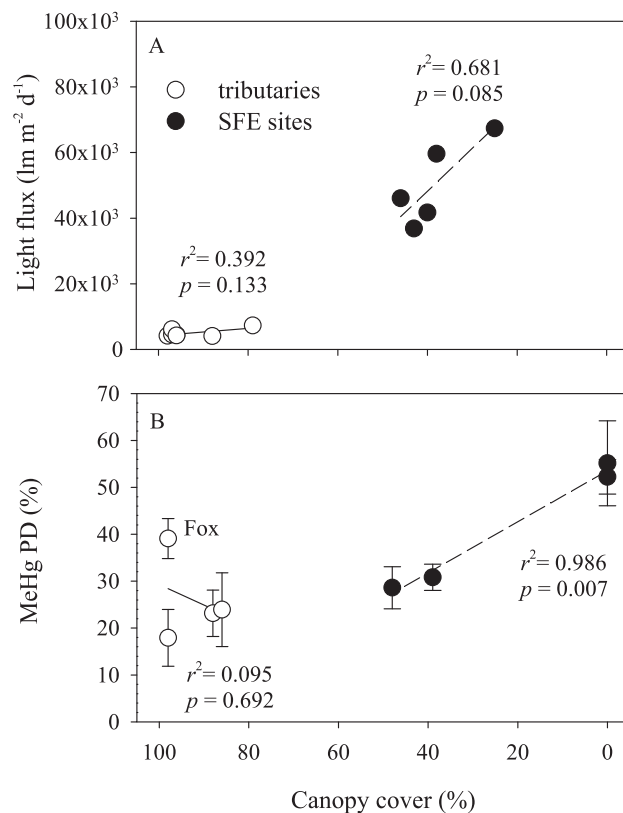
In a controlled experiment (Bergquist and Blum 2007) that exposed MeHg solutions with DOM to natural sunlight it was observed that the $\Delta^{199}Hg$ value increased gradually in the remaining MeHg in solution as MeHg PD progressed. Recent lake and marine studies (Bergquist and Blum 2007; Gehrke et al. 2011; Point et al. 2011) measuring stable Hg isotopes in food webs (e.g., fish and seabirds) employed the relationship from this controlled experiment (DOM at 1 or 10 mg C L$^{-1}$) and estimated the fraction of MeHg that had been photodegraded prior to bioaccumulation and trophic transfer. The situation in the stream network here represents an open environment, with water moving downstream being continuously photodegraded as it is coming into contact with an input of MeHg produced internally within the channels (Tsui et al. 2010). Thus, the $\Delta^{199}Hg_{MeHg}$ measured at one site should represent a bulk pool of MeHg that was derived from internally produced MeHg and partially photodegraded MeHg in sections upstream of the sampling point. We suggest the MIF values

can serve as an indicator of relative levels of MeHg PD along the drainage gradients studied here, as the results of MIF observed here are consistent with the expectation of a higher extent of MeHg PD in large stream channels.

We can infer that sunlight availability, which is strongly attenuated by canopy cover (Fig. 7A), is the main driver of MeHg PD across the stream network. It is interesting to note that the regression line between light flux (from mid–summer 2008) and canopy cover across SFE sites has a steeper slope than that between % MeHg PD and canopy cover (Fig. 7A,B). For example, the daily light flux varied by about 20 times between headwater streams and downstream channels, but MeHg PD varied only by a factor of $\sim$ 3 between them. The result may imply that as water moves downstream, other factors, such as increasing water depth and abundance of filamentous algal mats, may actually reduce sunlight or UV penetration in the water column and therefore lower the degree of MeHg PD, resulting in a nonlinear relationship between light flux and % MeHg PD along the drainage gradient.

It is important to note that higher MeHg PD in the larger streams may contribute to declining MeHg levels in both water and biota in the larger, more open sites (Figs. 2, 3). Like other undisturbed watersheds, algal photosynthesis in our study stream network is regulated by light availability, which is controlled by canopy shading (Finlay 2011; Finlay et al. 2011). For Hg cycling, light availability also influences in situ MeHg production (Tsui et al. 2010) as well as MeHg PD, as demonstrated in the present study. In other undisturbed watersheds, light patterns are generally similar across stream networks, so we might expect patterns of MeHg PD to be similar spatially, although the actual rates of MeHg PD may vary as a result of site-specific factors such as canopy cover, DOM, water turbidity, water depth, and water residence time in stream channels. Seasonality can also affect MeHg PD in all temperate ecosystems because of changing sunlight availability and canopy cover (especially for deciduous species), and, therefore, future studies will be needed to integrate different types of ecosystem variability into the development of predictive models for MeHg PD at the watershed scale.

At the same sites of sample collection, we found significant differences in $\Delta^{199}Hg_{MeHg}$ values between invertebrate FFGs, especially for scrapers (Fig. 5). Specifically, $\Delta^{199}Hg_{MeHg}$ values of scrapers are consistently higher (by up to 104%) than the values for the other three FFGs within individual sites (Fig. 5A–D). It is generally assumed that the dominant source of MeHg to the different groups of biota is the same at each site (Chasar et al. 2009; Tsui et al. 2009), but the contrast between scrapers and other FFGs indicates that in situ MeHg PD may actually vary between reservoirs within the same stream habitats. Since the scrapers were composed of armored caddisfly larvae that exclusively feed on algal cells (McNeely et al. 2006), the higher $\Delta^{199}Hg_{MeHg}$ for scrapers compared to other FFGs may imply that MeHg PD is elevated for MeHg associated with the algal biofilm. The higher MeHg PD associated with algal biofilms (either intracellular or extracellular) compared with the ambient environment is probably a consequence of algal biofilms being oriented to sunlight exposure to maximize photosynthesis. However, it is also
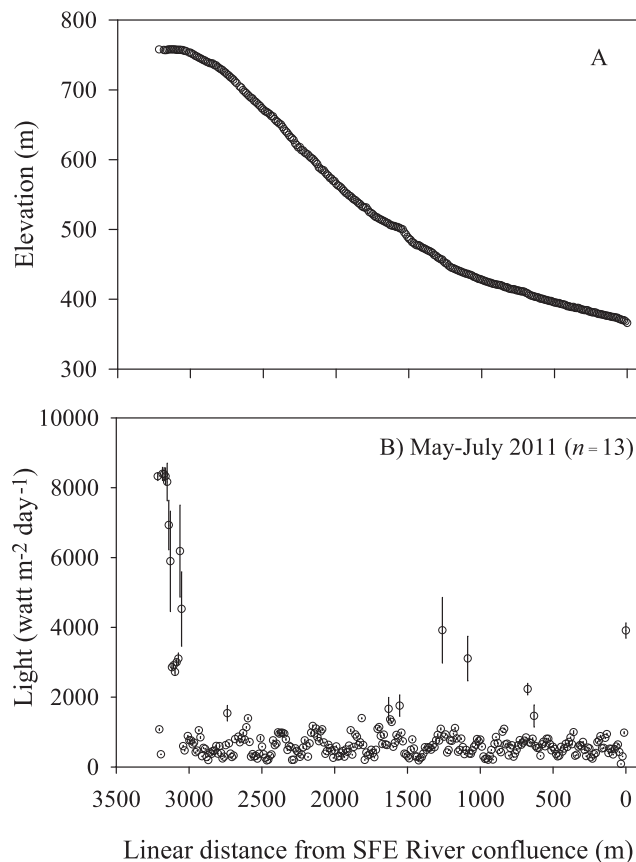


Fig. 8. Light levels along Fox Creek from its confluence with SFE River. (A) Elevation of measurement point and (B) mean light level from May through July 2011 ($n = 13$). Error bars in (B) are SD. Data provided by C. Bode (unpubl.).

possible that algal organic ligands or exudates might contribute to higher MeHg PD relative to the water column, corroborating previous laboratory experiments that showed a higher rate of Hg(II) photoreduction in the presence of algae (Deng et al. 2008). Thus, we infer that 'algal mediation' of MeHg PD may be proportionally more important in aquatic ecosystems with a high abundance of algae (e.g., biofilm, filamentous algae, and phytoplankton), but this hypothesis clearly requires further study.

Despite the generally increasing trend of $\Delta^{199}Hg_{MeHg}$ downstream, the $\Delta^{199}Hg_{MeHg}$ for four FFGs of invertebrates in Fox Creek (DA = 2.7 km²) was significantly higher than for other tributary streams and was somewhat unexpected (Fig. 5A–D) given the apparently high canopy cover (i.e., 98%) along this stream section. However, light models along this stream during the summer of 2011 indicated that there are meandering stream sections with a high openness (or sunlight levels) at the headwaters of Fox Creek (Fig. 8; C. Bode unpubl.). We speculate that this may support extensive MeHg PD after groundwater is discharged into the stream channel from springs. This is a plausible explanation because surface runoff is absent during the dry summer, and groundwater can contain trace amounts of MeHg (Stoor et al. 2006), despite being below the method detection limit ($< 20$ pg L$^{-1}$)

of this study. If this scenario is correct, then the process of MeHg PD in headwater streams results in bioaccumulated MeHg imprinted with very high $\Delta^{199}Hg_{MeHg}$, as observed in Fox Creek (Fig. 5A–D). This unexpected result further demonstrates the usefulness of stable Hg isotopes as a tool for integrating MeHg PD in natural ecosystems and shows that this method can detect the influence of MeHg PD even at those sites (e.g., upstream sections) situated away from sampling locations (e.g., downstream sections).

One of the limitations of the present study is that we had to estimate the isotope composition of bioaccumulated MeHg in stream insect larvae because of the large variation of $f_{MeHg}$ (i.e., from 0.25 to 1.00). In the future, refinement of methods for high yield separation ($> 90\%$) of large amounts of MeHg ($> 6$ ng) should allow direct high-precision measurement of the isotopic composition of MeHg from biological samples. If achieved, this analytical advancement will eliminate the uncertainty introduced by the isotopic estimation and thus provide a better estimate of MeHg PD in the environment.

This study and other recent studies employing stable Hg isotopes (Bergquist and Blum 2007; Gehrke et al. 2011; Point et al. 2011) demonstrate a unique approach for estimating MeHg PD in natural ecosystems without conventional incubation experiments (Sellers et al. 1996; Hammerschmidt and Fitzgerald 2006). The Hg isotope approach eliminates the use of MeHg addition (Hammerschmidt and Fitzgerald 2006) and the possibility of artificial attenuation of specific wavelengths of sunlight by the bottle materials used in incubation experiments (Black et al. 2012). Furthermore, the Hg isotope signals can be integrated over space and time, providing an estimate of average MeHg PD within a time frame (e.g., organismal life) and perhaps across boundaries in study ecosystems. We suggest that stable Hg isotopes can complement the results of conventional incubation experiments for MeHg PD studies, allowing us to better understand this biogeochemical process under different environmental conditions. This new approach allows us to interpret the relationship between odd-mass anomalies of Hg isotopes (i.e., $\Delta^{199}Hg$ or $\Delta^{201}Hg$) and rates of MeHg PD in different aquatic ecosystems, which can provide important information for applications such as mass balance measurements of MeHg in specific ecosystems. We suggest that stable Hg isotopes can be applied in many situations to gain a better understanding of ecosystem controls of MeHg PD, particularly in situations in which incubation experiments cannot be practically conducted, such as in fast-flowing streams, large and wide rivers, and subsurface layers and bottom waters of large lakes.

## References

Benoit, J. M., C. C. Gilmour, A. Heyes, R. P. Mason, and C. L. Miller. 2003. Geochemical and biological controls over methylmercury production and degradation in aquatic systems, p. 262–297. *In* Y. Cai and O. C. Braids [eds.], Biogeochemistry of environmentally important trace metals. ACS Symposium Series 835. American Chemical Society.

Bergquist, B. A., and J. D. Blum. 2007. Mass-dependent and -independent fractionation of Hg isotopes by photoreduction in aquatic systems. Science **318:** 417–420, doi:10.1126/science.1148050

Biswas, A., J. D. Blum, B. A. Bergquist, G. J. Keeler, and Z. Q. Xie. 2008. Natural mercury isotope variation in coal deposits and organic soils. Environ. Sci. Technol. **42:** 8303–8309, doi:10.1021/es801444b

Black, F. J., B. A. Poulin, and A. R. Flegal. 2012. Factors controlling the abiotic photo-degradation of monomethylmercury in surface waters. Geochim. Cosmochim. Acta **84:** 492–507, doi:10.1016/j.gca.2012.01.019

Bloom, N. 1989. Determination of picogram levels of methylmercury by aqueous phase ethylation, followed by cryogenic gas chromatography with cold vapour atomic fluorescence detection. Can. J. Fish. Aquat. Sci. **46:** 1131–1140, doi:10.1139/f89-147

Blum, J. D. 2011. Applications of stable mercury isotopes to biogeochemistry, p. 229–245. *In* M. Baskaran [ed.], Handbook of environmental isotope geochemistry. Springer.

———, and B. A. Bergquist. 2007. Reporting of variations in the natural isotopic composition of mercury. Anal. Bioanal. Chem. **388:** 353–359, doi:10.1007/s00216-007-1236-9

Bradley, P. M., and others. 2011. Spatial and seasonal variability of dissolved methylmercury in two stream basins in the eastern United States. Environ. Sci. Technol. **45:** 2048–2055, doi:10.1021/es103923j

Brigham, M. E., D. A. Wentz, G. R. Aiken, and D. P. Krabbenhoft. 2009. Mercury cycling in stream ecosystems. 1. Water column chemistry and transport. Environ. Sci. Technol. **43:** 2720–2725, doi:10.1021/es802694n

Chasar, L. C., B. C. Scudder, A. R. Stewart, A. H. Bell, and G. R. Aiken. 2009. Mercury cycling in stream ecosystems. 3. Trophic dynamics and methylmercury bioaccumulation. Environ. Sci. Technol. **43:** 2733–2739, doi:10.1021/es8027567

Deng, L., F. Wu, N. S. Deng, and Y. G. Zuo. 2008. Photoreduction of mercury(II) in the presence of algae, *Anabaena cylindrical*. Photochem. Photobiol. B Biol. **91:** 117–124, doi:10.1016/j.jphotobiol.2008.02.005

Finlay, J. C. 2004. Patterns and controls of lotic algal stable carbon isotope ratios. Limnol. Oceanogr. **49:** 850–861, doi:10.4319/lo.2004.49.3.0850

———. 2011. Stream size and human influences on ecosystem production in river networks. Ecosphere **2**, doi:10.1890/ES11-00071

———, J. M. Hood, M. P. Limm, M. E. Power, J. D. Schade, and J. R. Welter. 2011. Light-mediated thresholds in stream-water nutrient composition in a river network. Ecology **92:** 140–150, doi:10.1890/09-2243.1

FITZGERALD, W. F., D. R. ENGSTROM, R. P. MASON, AND E. A. NATER. 1998. The case for atmospheric mercury contamination in remote areas. Environ. Sci. Technol. **32:** 1–7, doi:10.1021/es970284w

GANTNER, N., H. HINTELMANN, W. ZHENG, AND D. C. G. MUIR. 2009. Variations in stable isotope fractionation of Hg in food webs of Arctic lakes. Environ. Sci. Technol. **43:** 9148–9154, doi:10.1021/es901771r

GEHRKE, G. E., J. D. BLUM, D. G. SLOTTON, AND B. K. GREENFIELD. 2011. Mercury isotopes link mercury in San Francisco Bay forage fish to surface sediments. Environ. Sci. Technol. **45:** 1264–1270, doi:10.1021/es103053y

HAMMERSCHMIDT, C. R., AND W. F. FITZGERALD. 2005. Methylmercury in mosquitoes related to atmospheric mercury deposition and contamination. Environ. Sci. Technol. **39:** 3034–3039, doi:10.1021/es0485107

———, AND ———. 2006. Photodecomposition of methylmercury in an arctic Alaskan lake. Environ. Sci. Technol. **40:** 1212–1216, doi:10.1021/es0513234

———, AND ———. 2010. Iron-mediated photochemical decomposition of methylmercury in an arctic Alaskan lake. Environ. Sci. Technol. **44:** 6138–6143, doi:10.1021/es1006934

HORVAT, M., L. LIANG, AND N. S. BLOOM. 1993. Comparison of distillation with other current isolation methods for the determination of methyl mercury compounds in low level environmental samples. Part II. Water. Anal. Chim. Acta **282:** 153–168, doi:10.1016/0003-2670(93)85348-N

KWON, S. Y., J. D. BLUM, M. J. CARVAN, N. BASU, J. A. HEAD, C. P. MADENJIAN, AND S. R. DAVID. 2012. Absence of fractionation of mercury isotopes during trophic transfer of methylmercury to freshwater fish in captivity. Environ. Sci. Technol. **46:** 7527–7534, doi:10.1021/es300794q

LAURION, I., M. VENTURA, AND J. CATALAN. 2000. Attenuation of ultraviolet radiation in mountain lakes: Factors controlling the among- and within-lake variability. Limnol. Oceanogr. **45:** 1274–1288, doi:10.4319/lo.2000.45.6.1274

LEHNHERR, I., AND V. L. ST. LOUIS. 2009. Importance of ultraviolet radiation in the photodemethylation of methylmercury in freshwater ecosystems. Environ. Sci. Technol. **43:** 5692–5698, doi:10.1021/es9002923

LIANG, L., AND N. S. BLOOM. 1993. Determination of total mercury by single-stage gold amalgamation with cold vapour atomic spectrometric detection. J. Anal. At. Spectrom. **8:** 591–594, doi:10.1039/JA9930800591

MCNEELY, C., S. M. CLINTON, AND J. M. ERBE. 2006. Landscape variation in C sources of scraping primary consumers in streams. J. N. Am. Benthol. Soc. **25:** 787–799, doi:10.1899/0887-3593(2006)025[0787:LVICSO]2.0.CO;2

PERROT, P., M. PASTUKHOV, V. N. EPOV, S. HUSTED, O. F. X. DONARD, AND D. AMOUROUX. 2012. Higher mass-independent isotope fractionation of methylmercury in the pelagic food web of Lake Baikal (Russia). Environ. Sci. Technol. **46:** 5902–5911, doi:10.1021/es204572g

PETERSON, S. A., J. VAN SICKLE, A. T. HERLIHY, AND R. M. HUGHES. 2007. Mercury concentration in fish from streams and rivers throughout the western United States. Environ. Sci. Technol. **41:** 58–65, doi:10.1021/es061070u

POINT, D., AND OTHERS. 2011. Methylmercury photodegradation influenced by sea-ice cover in Arctic marine ecosystems. Nat. Geosci. **4:** 188–194, doi:10.1038/ngeo1049

SELLERS, P., C. A. KELLY, J. W. M. RUDD, AND A. R. MACHUTCHON. 1996. Photodegradation of methylmercury in lakes. Nature **380:** 694–697, doi:10.1038/380694a0

SENN, D. B., E. J. CHESNEY, J. D. BLUM, M. S. BANK, A. MAAGE, AND J. P. SHINE. 2010. Stable isotope (N, C, Hg) study of methylmercury sources and trophic transfer in the northern Gulf of Mexico. Environ. Sci. Technol. **44:** 1630–1637, doi:10.1021/es902361j

STOOR, R. W., J. P. HURLEY, C. L. BABIARZ, AND D. E. ARMSTRONG. 2006. Subsurface sources of methyl mercury to Lake Superior from a wetland-forested watershed. Sci. Total Environ. **368:** 99–110, doi:10.1016/j.scitotenv.2005.10.019

TSUI, M. T. K., J. D. BLUM, S. Y. KWON, J. C. FINLAY, S. J. BALOGH, AND Y. H. NOLLET. 2012. Sources and transfers of methylmercury in adjacent river and forest food webs. Environ. Sci. Technol. **46:** 10957–10964, doi:10.1021/es3019836

———, AND J. C. FINLAY. 2011. Influence of dissolved organic carbon on methylmercury bioavailability across Minnesota stream ecosystems. Environ. Sci. Technol. **45:** 5981–5987, doi:10.1021/es200332f

———, ———, S. J. BALOGH, AND Y. H. NOLLET. 2010. In situ production of methylmercury within a stream channel in northern California. Environ. Sci. Technol. **44:** 6998–7004, doi:10.1021/es101374y

———, ———, AND E. A. NATER. 2009. Mercury bioaccumulation in a stream network. Environ. Sci. Technol. **43:** 7016–7022, doi:10.1021/es901525w

WALLACE, J. B., AND J. R. WEBSTER. 1996. The role of macroinvertebrates in stream ecosystem function. Annu. Rev. Entomol. **41:** 115–139, doi:10.1146/annurev.en.41.010196.000555

WIENER, J. G., D. P. KRABBENHOFT, G. H. HEINZ, AND A. M. SCHEUHAMMER. 2003. Ecotoxicology of mercury, p. 409–463. *In* D. J. Hoffman, B. A. Rattner, G. A. Burton, and J. Cairns [eds.], Handbook of ecotoxicology. CRC.

ZHANG, T., AND H. HSU-KIM. 2010. Photolytic degradation of methylmercury enhanced by binding to natural organic ligands. Nat. Geosci. **3:** 473–476, doi:10.1038/ngeo892